Cavity-Enhanced Rydberg Atom Microwave Receiver

Bang Liu[1,2], Li-Hua Zhang[1,2], Qi-Feng Wang[1,2], Yu Ma[1,2], Tian-Yu Han[1,2], Zong-Kai Liu[1,2], Zheng-Yuan Zhang[1,2], Shi-Yao Shao[1,2], Jun Zhang[1,2], Qing Li[1,2], Han-Chao Chen[1,2], Yu-Long Han[3], Dong-Sheng Ding[1,2*], and Bao-Sen Shi[1,2]

[1]*Key Laboratory of Quantum Information, University of Science and Technology of China, Hefei 230026, China*
[2]*Synergetic Innovation Center of Quantum Information and Quantum Physics, University of Science and Technology of China, Hefei 230026, China*
[3]*General Education & Foreign Language College, Anhui Institute of Information Technology, Wuhu 241003, China*

(Received 25 December 2024; accepted manuscript online 7 April 2025)

Developing microwave electric field sensing based on Rydberg atoms has received significant attention due to its unique advantages. However, achieving effective coupling between Rydberg atoms and the microwave electric field in the sensing process is a challenging problem that greatly impacts the sensitivity. To address this, we propose using a microwave resonant cavity to enhance the effective coupling between the Rydberg atoms and the microwave electric field. In our experiment, Rydberg atoms are prepared via a three-photon excitation scheme, and the electric fields are measured without and with a microwave cavity in which the vapor cell is placed inside, respectively. As a result, we achieved an 18 dB enhancement of power sensitivity by adding the cavity, which is an effective enhancement in electric field pulse signal detection. This experimental testing provides a promising direction for enhancing the sensitivity of Rydberg atomic electric field sensors and paves the way for their application in precision electric field measurements.

DOI: 10.1088/0256-307X/42/5/053201 CSTR: 32039.14.0256-307X.42.5.053201

Introduction. Microwave (MW) electric field sensing based on Rydberg atoms offers the ability to achieve high sensitivity as the large polarizability of Rydberg atoms[1] makes them sensitive to external electric fields.[2,3] Through the control of a narrow band laser field, its energy levels can be tailored to match the desired MW frequency range, and providing a non-destructive measurement. This flexibility allows for the development of a wide range of sensors that can operate at different frequencies,[4–7] making them suitable for various applications, such as metrology,[8,9] sensing,[10,11] and communication.[12–15]

Recently, different schemes have been proposed to achieve electric field measurements based on the electromagnetically induced transparency (EIT) effect of Rydberg atoms,[16,17] and high sensitivity has been obtained with different protocols.[2,3,18] The rich energy level structures of the Rydberg atoms have also been used to achieve measurements of RF electric fields in the kHz–THz range.[19–22] The practical applications of Rydberg atomic electric field measurements have been actively explored, and the great potential of such measurements has been demonstrated.[23–26]

However, in order to better promote the application of Rydberg atoms in MW electric field measurements, it is particularly important to improve the sensitivity of Rydberg atoms for MW sensing. Although the quantum projection noise limit sensitivity of Rydberg atoms is theoretically advantageous compared to that of conventional antennas,[11,13] it is still unable to surpass the sensitivity of conventional antennas in practice due to experimental conditions. One of the core problems is how to solve the effective coupling between the Rydberg atoms and the MW electric field.[20,27–31] Conventional MW antennas have directional gain by collecting the MW electric field in a certain directional range for measurement, while the sensing component of the Rydberg atomic electric field measurement system is a glass vapor cell, which does not have directional gain. Additionally, the external MW electric field tends to disperse in free space, and the spatial area in which Rydberg atoms exist within the vapor cell is very limited due to constraints imposed by the excitation laser. This makes it challenging to effectively couple the Rydberg atoms with the external MW electric field, resulting in significant insertion loss and a substantial reduction in sensitivity for Rydberg atomic electric field measurements.

Here, we report an experiment of cavity enhanced Rydberg atoms MW receiver. Coupling Rydberg atoms with a MW cavity allows for strong interaction between MW radiation and Rydberg atoms, resulting in increased sensitivity to small changes in the MW signal. This can be theoretically explained by the MW resonator model. Experimentally, we have achieved an 18 dB power sensitivity enhancement for the measurement of electric field with a MW cavity. This enables more accurate and precise measurements and builds the foundation for further improvement of the Rydberg atomic electric field sensing performance.

*Corresponding author. Email: dds@ustc.edu.cn
© 2025 Chinese Physical Society and IOP Publishing Ltd. All rights, including for text and data mining, AI training, and similar technologies, are reserved.

Experiment Setup. We use a Cesium atom vapour cell in our experiments to demonstrate electric field sensing. The energy level structure of atoms and the experimental setup are shown in Figs. 1(a) and 1(b). We use a three-photon excitation scheme to excite atoms from the ground state to the Rydberg state,[32] with 852 nm probe light driving the transition of $|1\rangle \rightarrow |2\rangle$ ($|6S_{1/2}\rangle \rightarrow |6P_{3/2}\rangle$), 1470 nm laser driving the transition of $|2\rangle \rightarrow |3\rangle$ ($|6P_{3/2}\rangle \rightarrow |7S_{1/2}\rangle$), and 780 nm coupling light driving the transition of $|3\rangle \rightarrow |4\rangle$ ($|7S_{1/2}\rangle \rightarrow |55P_{3/2}\rangle$), corresponding to the Rabi frequencies $\Omega_{\rm p}$, $\Omega_{\rm d}$, and $\Omega_{\rm c}$, respectively. In the experimental setup, the probe light is divided into two beams to pass through the atomic vapor cell, while the dressing and coupling lights propagate in the opposite direction to one of the probe light beams to reduce the Doppler broadening effect. The length of vapor cell is 7 cm. The probe light is focused into the cell ($1/e^2$-waist radius of approximately 200 μm) with a probe intensity of 64 μW. The dressing and coupling lights are focused into the cell ($1/e^2$-waist radius of approximately 500 μm) and the powers are 16.8 mW and 1.5 W respectively. Finally, the two beams are received by a balanced photoelectric detector for differential amplification measurement.

The vapor cell is placed into a metal MW resonant cavity made of oxygen-free copper, and the MW field is fed through an external sub-miniature-A (SMA) port to drive the transition of $|4\rangle \rightarrow |5\rangle$ ($|55P_{3/2}\rangle \rightarrow |54D_{5/2}\rangle$) with Rabi frequency $\Omega_{\rm MW}$. The length of the microwave cavity is 76 mm and the diameter is 41 mm. At the same time, two small holes need to be opened at both ends of the resonant cavity to allow the laser to pass through. Another two small holes are located at the center of bottom side spaced 1 cm apart, and the diameter of the holes is 1.5 mm. While, this leads to a decrease in the Q-factor of the resonant cavity. Efficient coupling between the Rydberg atoms and the cavity mode is essential for achieving high sensitivity. This requires careful consideration of factors such as atom-cavity detuning, cavity mode volume, and the positioning of the atomic ensemble relative to the cavity field. In our setup, we strategically place the atomic cell in the center of the cavity to maximize the coupling strength.

Results. First we simulated the MW electric field distribution in the cavity, as shown in Fig. 2(a). It is observed that the maximum of field strength is at the center of the cavity. To take this advantage, we position the atomic vapor cell inside the cavity and utilize lasers to excite the atoms to the Rydberg state precisely at the center. This arrangement ensures that the induced field strength is maximized. Additionally, we conducted a simulation of the s_{11} parameter for the MW cavity and compared it with the actual measurement using a vector network analyzer, as depicted in Fig. 2(b). The simulation results indicate that the resonance of the MW cavity is most pronounced at 4.485 GHz, which aligns with our experimental measurements. Nevertheless, the measured s_{11} parameter is relatively low with a value of −13 dB. This reduction can be attributed to both the machining process and the presence of the atomic vapor cell within the cavity. In particular, the input and output ports on the cavity are not precisely impedance-matched to the cavity. This results in the microwaves not forming enhanced reflections in the cavity, thus reducing the s_{11} parameter of the cavity. Moreover, the inclusion of an atomic vapor cell within the cavity increases the dielectric permittivity of the cavity, further increasing the losses in the cavity and thus reducing the overall performance of the cavity.

After adding a MW cavity and comparing it with a general horn antenna, we investigated the EIT spectral characteristics. The results are presented in Fig. 1(c). In the absence of an electric field, the EIT spectrum is represented by the blue line, exhibiting a transmission peak. When a MW electric field is applied using the horn antenna (close to the vapor cell), a slight broadening of the EIT spectrum is observed. This broadening occurs because the electric field strength is not sufficient to induce splitting in the EIT spectrum. On the other hand, when a MW resonant cavity is added and supplied with microwaves of the same power, the EIT spectrum clearly splits. This splitting is a result of the stronger coupling between the

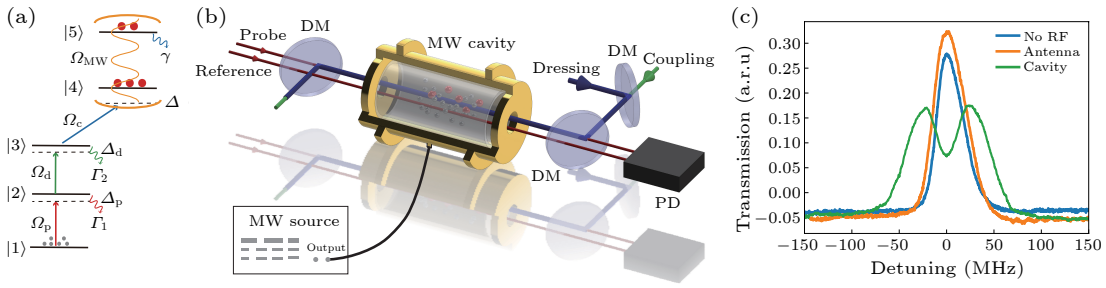

Fig. 1. (a) Energy-level diagram of three photon Rydberg-EIT. The probe laser is resonant with transition of $|1\rangle \rightarrow |2\rangle$ ($|6S_{1/2}\rangle \rightarrow |6P_{3/2}\rangle$) with Rabi frequency of $\Omega_{\rm p}$. The dressing laser drives the transition of $|2\rangle \rightarrow |3\rangle$ ($|6P_{3/2}\rangle \rightarrow |7S_{1/2}\rangle$) with $\Omega_{\rm d}$. The coupling laser drives the transition of $|3\rangle \rightarrow |4\rangle$ ($|7S_{1/2}\rangle \rightarrow |55P_{3/2}\rangle$) with $\Omega_{\rm c}$. The resonant frequency of the MW cavity is 4.485 GHz, which couples with electric fields at transition of $|4\rangle \rightarrow |5\rangle$ ($|55P_{3/2}\rangle \rightarrow |54D_{5/2}\rangle$) with $\Omega_{\rm MW}$. (b) Schematic of experimental setup. DM: dichroic mirror. PD: photodetector. (c) The EIT spectra of probe light with or without MW cavity. The horizontal coordinate is the detuning of the coupling light. The blue line is the transmission of probe light without MW cavity, showing an EIT peak. The green line is the EIT spectra with MW cavity, which has two peaks caused by Autler-Townes splitting. The antenna has a gain of 15 dB and is placed 4 cm from the vapor cell.

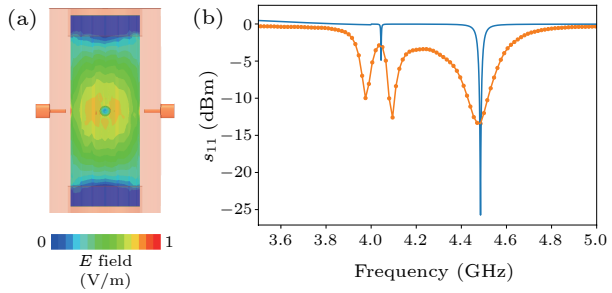

Fig. 2. (a) Electric field distribution inside the microwave cavity. (b) s_{11} parameter for the microwave cavity. The blue curve is the result of a theoretical simulation, and orange data points are the results of experimental measurements.

MW electric field inside the cavity and the Rydberg atoms. Moreover, the presence of the MW cavity enhances the coupling strength. In experiment, we set $\Delta_{\rm p} = \Delta_{\rm d} = 0$. The transmission of the probe light in the experiment corresponds to the imaginary part of the density matrix element ρ_{21}. The steady-state solution of the system $\rho_{21}(\Delta_{\rm c})$ can be obtained by solving the Lindblad equation, which is the EIT spectrum shown in Fig. 1(c). In the absence of a MW electric field, the three-photon EIT phenomenon occurs, which is due to the dark state of the system. Whereas, with the MW electric field applied and ignoring $\Omega_{\rm p}$ and $\Omega_{\rm c}$, the dark state of the system splits under the MW dressing and the energy splitting is [11,12]

$$\Delta E \propto \hbar\Omega_{\rm MW}, \tag{1}$$

which corresponds to the splitting of the EIT spectrum in Fig. 1(c), where $\Omega_{\rm MW} = \mu E_{\rm MW}/\hbar$ is the coupling strength of MW electric field with Rydberg atoms.

When an input electric field is given to the MW cavity, the circulating power in the cavity becomes larger due to the resonance effect of the cavity, making the electric field sensed by the atoms larger. When input energy is $W_{\rm in}$, we can obtain

$$W_{\rm in} = W_{\rm out} + W_{\rm r} + W_{\rm d} + W_{\rm dL}, \tag{2}$$

where $W_{\rm out}$ is the energy output from the cavity, $W_{\rm r}$ is the energy reflected back from the cavity, $W_{\rm d}$ and $W_{\rm dL}$ are the energy lost in the inner wall of the cavity and the energy lost in the connecting wires and ports, respectively. Using the definition of the S-parameters, we can obtain

$$1 = |s_{21}|^2 + |s_{11}|^2 + \frac{W_{\rm d} + W_{\rm dL}}{W_{\rm in}}. \tag{3}$$

Using the definition of the Q-factor of the resonator $Q = W_{\rm s}/(W_{\rm d} + W_{\rm dL})$, the energy stored in the cavity $W_{\rm s}$ is

$$\frac{W_{\rm s}}{W_{\rm in}} = (1 - |s_{11}|^2 - |s_{21}|^2)Q, \tag{4}$$

where s_{11}, s_{21} are S-parameters, which characterize the microwave reflection and transmission properties of the cavity, respectively. So we can define the enhanced factor of the cavity $F = (1 - |s_{11}|^2 - |s_{21}|^2)Q$, which will enhanced the sensitivity of Rydberg atomic electric field metrology.

For the electric field in the cavity, we can approximate that it is uniform along the direction of the cavity. We assume that the electric field inside the cavity is symmetrically distributed, with its maximum intensity at the center. By integrating the electric field strength within the cavity, we can derive the following:

$$W_{\rm s} = \frac{1}{4}\varepsilon_0 \pi a^2 d |E_{\rm MW}|^2, \tag{5}$$

where a is radius of cavity, d is the length of cavity, $E_{\rm MW}$ is the electric field strength at the center, and ε_0 is the permittivity of free space. Furthermore, the coupling strength of MW electric field inside cavity with Rydberg atoms is

$$\Omega_{\rm MW} = \frac{\mu E_{\rm MW}}{\hbar} = \frac{2\mu}{\hbar}\left[\frac{(1-|s_{11}|^2-|s_{21}|^2)W_{\rm in}Q}{\varepsilon_0 \pi a^2 d}\right]^{1/2}. \tag{6}$$

We exploit the resonance enhancement of the MW cavity to achieve an improved measurement of the MW. The results are presented in Fig. 3. We employed the superheterodyne measurement technique to apply a strong local oscillation (LO) and a weak signal MW with a slight detuning from the LO. It was observed that the EIT spectrum is modulated by the beat frequency of the LO and the signal. The system's beat-frequency response was measured using a spectrum analyzer, and the response intensity corresponds to the intensity of the signal under measurement. As depicted in Fig. 3(a), the blue data represents the system's response with the inclusion of the MW cavity, while the orange data corresponds to the response without the cavity. It is evident that the dynamic range of both cases

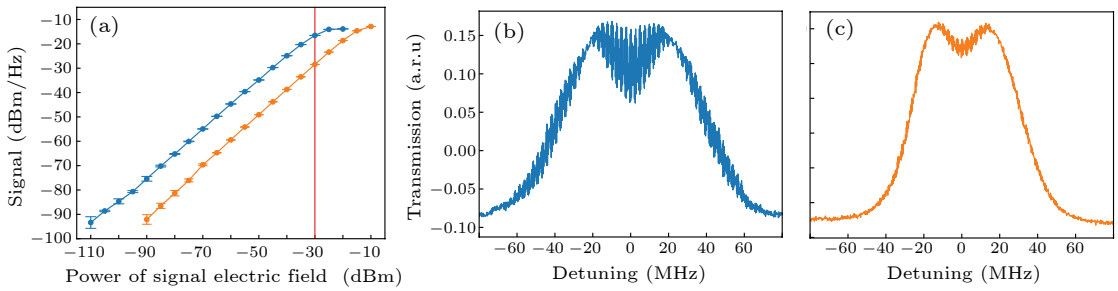

Fig. 3. (a) Measured beat-frequency signal strength at different signal electric field powers, showing a linear response over a range of powers. The blue line is the measured data with a resonant microwave cavity, the orange one is without a cavity. The red line marks the measured data for cavity (blue) and no-cavity (orange) with $P_{\rm sig} = -30$ dBm signal input. (b) Measured the EIT spectra when applied a $P_{\rm sig} = -30$ dBm signal field with a cavity. (c) Measured the EIT spectra when applied a $P_{\rm sig} = -30$ dBm signal field without a cavity.

is approximately equal, measuring around 75 dB. However, with the addition of the MW cavity, the minimum measurable MW power can be as low as −110 dBm, which is approximately 18 dB stronger compared to the case without the cavity.

Figures 3(b) and 3(c) illustrate the EIT spectral features at an input power of −30 dBm for both scenarios. It is evident that the addition of the MW cavity leads to a more pronounced modulation of the EIT spectra. This can be attributed to the enhanced MW resonance cavity. However, it should be noted that when the power of the signal electric field becomes too large, the system response deviates from linearity. This occurs due to the violation of the condition that the signal electric field should be significantly smaller than the intrinsic vibration field in the superheterodyne measurement scheme.

Finally, we have demonstrated the reception of the system using square-wave modulated MW signals to verify the performance of sensing MW electric fields. Instead of utilizing the superheterodyne measurement scheme, we directly observe the change in the transmission of the probe light. To do this, we applied a square-wave modulated MW signal with a modulation frequency of 1 kHz through a signal source. The signal was then received and demodulated by our Rydberg atom system. Measurement results are shown in Fig. 4.

By utilizing a MW resonant cavity, we are able to achieve a significantly larger signal-to-noise ratio (blue curve) compared to the scenario without a cavity (orange curve) as shown in Fig. 4. This enhancement in the signal-to-noise ratio is particularly beneficial in reception of weaker signals. In fact, with the addition of a cavity, the signal-to-noise ratio of the received square-wave modulated signal is boosted by a factor of $\beta = 10.8$. Moreover, the use of the cavity also results in a reduction in the bit error rate during the reception of digitally modulated signals.

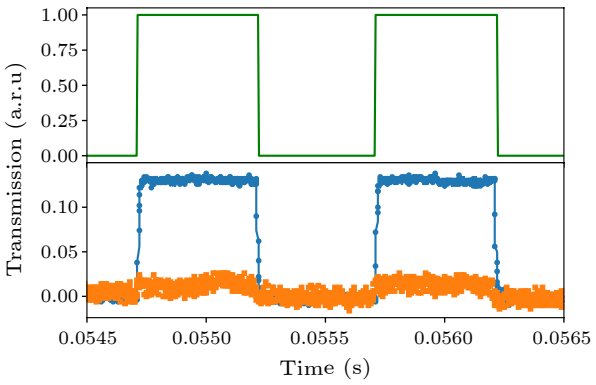

Fig. 4. Comparison of the real-time response spectra of the Rydberg atom system with and without a cavity under the application of a square-wave modulation signal with the modulation frequency of 1 kHz, the modulation depth of 30%, and $P = -30$ dBm. The green curve is the modulated signal of the carrier, the blue curve is the signal demodulated from the Rydberg atoms with the cavity, and the orange curve is that without the cavity.

Discussion. Due to the small volume of the laser excitation in the atomic vapor cell, typically only a few hundred microns, the effective receiving area of the Rydberg atomic electric field sensor is indeed limited. This small effective area results in reduced sensitivity to the electric field being measured. The MW resonant cavity performs two primary functions. Firstly, it allows for the matching of the atoms by compressing the spatial volume of the electric field within the cavity. This compression ensures efficient interaction between the MW electric field and the Rydberg atoms. Secondly, the resonance effect of the MW cavity is utilized to enhance the interaction between the MW electric field and the Rydberg atoms. This enhancement further improves the sensitivity of the measured electric field. [33]

The performance of the resonant cavity plays a crucial role in this scenario. In experimental setups, a MW cavity with a relatively high Q-factor of approximately 130 is typically employed. The Q-factor can be further enhanced by reducing the cavity's volume and using low-loss dielectric materials. By achieving a Q-factor of 4×10^5, the power sensitivity can reach as low as −180 dBm/Hz, surpassing the thermal noise limit of conventional antennas. Currently, with the use of superconducting metal surfaces as mirrors for resonant cavities, Q-factors as high as 10^7–10^9 have been achieved. [34,35] Therefore, by combining Rydberg atoms with resonant cavities, it becomes feasible to perform measurements of extremely weak MW electric fields. Meanwhile, processing and fabrication of high Q-factor microwave cavities and achieving effective coupling with Rydberg atoms will be challenging problems. In addition the reduced cavity size will limit the size of the vapor cell, thus affecting the number of Rydberg atoms used for sensing, which needs to be weighed.

While MW cavities can significantly enhance sensitivity, it is important to note that their resonant frequency tends to be narrow. Therefore, it is crucial to ensure that the input electric field strictly matches the cavity's resonance frequency. Otherwise, the performance of the cavity will be greatly compromised. In the future, there may be possibilities to broaden the operating bandwidth by adjusting the length of the MW cavity, allowing for greater flexibility in matching the resonant frequency.

Conclusion. We have successfully demonstrated an experiment of enhanced interaction between Rydberg atoms and the MW electric field by utilizing the resonance effect of the MW cavity. Through the investigation of the effective coupling between Rydberg atoms and the electric field within the cavity, we have achieved an 18 dB increase in power sensitivity. Moreover, this enhancement effect has allowed us to improve the signal-to-noise ratio in signal demodulation, which is crucial in advancing the practical application of Rydberg atom-based electric field sensors.

There are several potential avenues for further improvement in the future. One possibility is to fabricate cavities with higher Q-factors, which would enhance the measurement sensitivity even more. Additionally, it would be worthwhile to explore the dynamics evolution of Ryd-

berg atoms under strong coupling conditions. Furthermore, we can also investigate applications of atomic sensors in areas requiring extremely high measurement sensitivities, such as dark matter detection. Overall, our results not only contribute to the advancement of Rydberg atom-based electric field sensor systems, but also open up new possibilities for their utilization in a range of scientific and technological applications.[36–38]

Acknowledgements. We are grateful to Prof. Xiao-Ming Liu from Anhui Normal University for fruitful discussions about cavity designing. We acknowledge the fundings from National Key R&D Program of China (Grant No. 2022YFA1404002), National Natural Science Foundation of China (Grant Nos. T2495253, U20A20218, 61525504, and 61435011), Anhui Initiative in Quantum Information Technologies (Grant No. AHY020200), Major Science and Technology Projects in Anhui Province (Grant No. 202203a13010001), and Youth Innovation Promotion Association of the Chinese Academy of Sciences (Grant No. 2018490). Yu-Long Han acknowledges the fundings from Anhui Provincial Department of Education (Grant No. YQZD2024061) and Research Program of Higher Education Institutions in Anhui Province (Grant No. 2024AH050645).

References

[1] Adams C S, Pritchard J D, and Shaffer J P 2019 *J. Phys. B: At. Mol. Opt. Phys.* **53** 012002
[2] Ding D S, Liu Z K, Shi B S, Guo G C, Molmer K, and Adams C S 2022 *Nat. Phys.* **18** 1447
[3] Jing M Y, Hu Y, Ma J, Zhang H, Zhang L J, Xiao L T, and Jia S T 2020 *Nat. Phys.* **16** 911
[4] Hu J L, Li H Q, Song R, Bai J X, Jiao Y C, Zhao J M, and Jia S T 2022 *Appl. Phys. Lett.* **121** 014002
[5] Simons M T, Artusio-Glimpse A B, Holloway C L, Imhof E, Jefferts S R, Wyllie R, Sawyer B C, and Walker T G 2021 *Phys. Rev. A* **104** 032824
[6] Liu X H, Liao K Y, Zhang Z X, Tu H T, Bian W, Li Z Q, Zheng S Y, Li H H, Huang W, Yan H, and Zhu S L 2022 *Phys. Rev. Appl.* **18** 054003
[7] Berweger S, Prajapati N, Artusio-Glimpse A B, Rotunno A P, Brown R, Holloway C L, Simons M T, Imhof E, Jefferts S R, Kayim B N, Viray M A, Wyllie R, Sawyer B C, and Walker T G 2023 *Phys. Rev. Appl.* **19** 044049
[8] Anderson D A, Sapiro R E, and Raithel G 2021 *IEEE Trans. Antennas Propag.* **69** 5931
[9] Holloway C L, Simons M T, Gordon J A, Dienstfrey A, Anderson D A, and Raithel G 2017 *J. Appl. Phys.* **121** 233106
[10] Jia F D, Liu X B, Mei J, Yu Y H, Zhang H Y, Lin Z Q, Dong H Y, Zhang J, Xie F, and Zhong Z P 2021 *Phys. Rev. A* **103** 063113
[11] Fan H Q, Kumar S, Sedlacek J, Kubler H, Karimkashi S, and Shaffer J P 2015 *J. Phys. B: At. Mol. Opt. Phys.* **48** 202001
[12] Liu B, Zhang L H, Liu Z K, Deng Z, Ding D S, Shi B S, and Guo G C 2023 *Electromagn. Sci.* **1** 1
[13] Fancher C T, Scherer D R, John M C S, and Marlow B L S 2021 *IEEE Trans. Quantum Eng.* **2** 1
[14] Holloway C L, Simons M T, Haddab A H, Gordon J A, Anderson D A, Raithel G, and Voran S 2021 *IEEE Antennas Propag. Mag.* **63** 63
[15] Anderson D A, Sapiro R E, and Raithel G 2021 *IEEE Trans. Antennas Propag.* **69** 2455
[16] Mohapatra A K, Jackson T R, and Adams C S 2007 *Phys. Rev. Lett.* **98** 113003
[17] Sedlacek J A, Schwettmann A, Kubler H, Low R, Pfau T, and Shaffer J P 2012 *Nat. Phys.* **8** 819
[18] Cai M H, Xu Z S, You S H, and Liu H P 2022 *Photonics* **9** 250
[19] Jau Y Y and Carter T 2020 *Phys. Rev. Appl.* **13** 054034
[20] Meyer D H, Kunz P D, and Cox K C 2021 *Phys. Rev. Appl.* **15** 014053
[21] Downes L A, MacKellar A R, Whiting D J, Bourgenot C, Adams C S, and Weatherill K J 2020 *Phys. Rev. X* **10** 011027
[22] Liu B, Zhang L H, Liu Z K, Zhang Z Y, Zhu Z H, Gao W, Guo G C, Ding D S, and Shi B S 2022 *Phys. Rev. Appl.* **18** 014045
[23] Liu Z K, Zhang L H, Liu B, Zhang Z Y, Guo G C, Ding D S, and Shi B S 2022 *Nat. Commun.* **13** 1997
[24] Zhang L H, Liu Z K, Liu B, Zhang Z Y, Guo G C, Ding D S, and Shi B S 2022 *Phys. Rev. Appl.* **18** 014033
[25] Anderson D A, Sapiro R E, and Raithel G 2020 *IEEE Aerosp. Electron. Syst. Mag.* **35** 48
[26] Meyer D H, Cox K C, Fatemi F K, and Kunz P D 2018 *Appl. Phys. Lett.* **112** 211108
[27] Morgan A A and Hogan S D 2020 *Phys. Rev. Lett.* **124** 193604
[28] Hogan S D, Agner J A, Merkt F, Thiele T, Filipp S, and Wallraff A 2012 *Phys. Rev. Lett.* **108** 063004
[29] Walker D M, Brown L L, and Hogan S D 2022 *Phys. Rev. A* **105** 022626
[30] Holloway C L, Prajapati N, Artusio-Glimpse A B, Berweger S, Simons M T, Kasahara Y, Alu A, and Ziolkowski R W 2022 *Appl. Phys. Lett.* **120** 204001
[31] Yang K, Mao R Q, He L, Yao J W, Li J B, Sun Z S, and Fu Y Q 2023 *EPJ Quantum Technol.* **10** 23
[32] Thaicharoen N, Moore K R, Anderson D A, Powel R C, Peterson E, and Raithel G 2019 *Phys. Rev. A* **100** 063427
[33] Santamaria-Botello G, Verploegh S, Bottomley E, and Popovic Z 2022 arXiv:2209.00908
[34] Kuhr S, Gleyzes S, Guerlin C, Bernu J, Hoff U B, Deleglise S, Osnaghi S, Brune M, Raimond J M, Haroche S, Jacques E, Bosland P, and Visentin B 2007 *Appl. Phys. Lett.* **90** 164101
[35] Suleymanzade A, Anferov A, Stone M, Naik R K, Oriani A, Simon J, and Schuster D 2020 *Appl. Phys. Lett.* **116** 104001
[36] Gue J, Hees A, Lodewyck J, Le Targat R, and Wolf P 2023 *Phys. Rev. D* **108** 035042
[37] Bradley R, Clarke J, Kinion D, Rosenberg L J, van Bibber K, Matsuki S, Muck M, and Sikivie P 2003 *Rev. Mod. Phys.* **75** 777
[38] Engelhardt G, Bhoonah A, and Liu W V 2023 arXiv:2304.05863